ChemPubSoc Europe

DOI: 10.1002/chem.201503685

CHEMISTRY
A European Journal
Full Paper

Hydrocarbon Separation

Influence of Solvent-Like Sidechains on the Adsorption of Light Hydrocarbons in Metal–Organic Frameworks

Andreas Schneemann,[a] Eric D. Bloch,[b, c] Sebastian Henke,[a] Philip L. Llewellyn,[d] Jeffrey R. Long,*[b] and Roland A. Fischer*[a]

Abstract: A variety of strategies have been developed to adsorb and separate light hydrocarbons in metal–organic frameworks. Here, we present a new approach in which the pores of a framework are lined with four different C3 sidechains that feature various degrees of branching and saturation. These pendant groups, which essentially mimic a low-density solvent with restricted degrees of freedom, offer tunable control of dispersive host–guest interactions. The performance of a series of frameworks of the type Zn_2(fu-bdc)$_2$(dabco) (fu-bdc^{2-} = functionalized 1,4-benzenedicarboxylate; dabco = 1,4-diazabicyclo[2.2.2]octane), which feature a pillared layer structure, were investigated for the adsorption and separation of methane, ethane, ethylene, and acetylene. The four frameworks exhibit low methane uptake, whereas C2 hydrocarbon uptake is substantially higher as a result of the enhanced interaction of these molecules with the ligand sidechains. Most significantly, the adsorption quantities and selectivity were found to depend strongly upon the type of sidechains attached to the framework scaffold.

Introduction

The light hydrocarbons methane, ethane, ethylene, and acetylene are typically obtained as mixtures from either natural gas or the steam cracking of naphtha.[1] An extremely cost-intensive portion of the production of these important chemicals thus lies in their separation from the product stream.[2] The most widely employed method for performing such a separation is cryogenic distillation, a process that, owing to the low boiling points and similar physical properties of these molecules, must be carried out at low temperatures and high pressures. A potentially more energy-efficient alternative involves a higher-temperature adsorptive separation by using porous materials.[2–3] A specific class of materials that have been thoroughly investigated for adsorption-based separations, in addition to numerous other applications, are metal–organic frameworks (MOFs).[4] These materials are composed of metal cations or clusters connected by organic linkers (predominantly carboxylate or N-coordinating, multidentate ligands) to create often porous, architecturally robust three-dimensional networks. The highly tunable structures that result possess a large range of surface areas, pore geometries, and surface functionalities.[5]

To differentiate hydrocarbons within a MOF, the two most commonly investigated strategies have been the utilization of coordinatively unsaturated metal sites[6] and/or the tuning of pore size and geometry.[7] A specific example of the former is the metal–organic framework Fe_2(dobdc) (dobdc^{4-} = 2,5-dioxido-1,4-benzenedicarboxylate; also known as CPO-27-Fe or Fe-MOF-74).[6b] This material displays high selectivity for a number of hydrocarbon separations based on the different binding affinities of hydrocarbons to the exposed Fe^{2+} cations of the framework. In tuning pore size and shape for a given separation, discrimination of different hydrocarbons is achieved by taking advantage of the distinctive kinetic diameters of the adsorbent molecules, similar to the separation mechanism in zeolites.[8] Alternatively, sharp angular features attainable within the pores of a MOF, but not in zeolites, can be used to engender shape-based separations for mixtures of alkane isomers.[9] The combination of open metal sites and size/shape-selectivity has also been adopted. In this approach, side groups[10] or interpenetration[11] can be used to tune pore size, which leads to better confinement of molecules in the pores, whereas open metal sites located on the pore surface lead to a stronger affinity towards specific guests.

[a] A. Schneemann, Dr. S. Henke, Prof. Dr. R. A. Fischer
Lehrstuhl für Anorganische Chemie II, Organometallics and Materials Chemistry
Ruhr-Universität Bochum
Universitätsstr. 150, 44801 Bochum (Germany)
E-mail: Roland.Fischer@rub.de

[b] Dr. E. D. Bloch, Prof. Dr. J. R. Long
Department of Chemistry
University of California, Berkeley
Berkeley 94720 California (USA)
E-mail: jrlong@berkeley.edu

[c] Dr. E. D. Bloch
Department of Chemistry and Chemical Biology
Harvard University
12 Oxford Street, Cambridge 02138 Massachusetts (USA)

[d] Dr. P. L. Llewellyn
Aix-Marseille University, CNRS, MADIREL (UMR 7246)
Centre Scientifique de St. Jérôme
13397 Marseille cedex 20 (France)

Supporting information for this article is available on the WWW under http://dx.doi.org/10.1002/chem.201503685.

Although pendant side groups can be used to tune the shape and size of pores in MOFs, they may potentially also be useful for introducing specific adsorbent–adsorbate interactions. For example, the separation of $CH_4/CO_2/N_2$ mixtures was studied in UiO-66 materials that contained functional groups that both altered pore size and also integrated new interaction sites into the MOF, which thus modulated selectivity (e.g., by introducing NH_2 or NO_2 groups).[12] However, it may be even more desirable to prevent the uptake of certain guest molecules by introducing rather bulky substituents that gate the channels by interacting more strongly with each other than with adsorbent molecules.[13] This strategy has been used, for example, to impart selectivity towards polar molecules in a material in which sidechains form strong hydrogen bonds with each other.[14]

Along these lines, we decided to utilize flexible sidechains covalently bonded to the ligand backbone that can rotate and rearrange within the pore. These pendant groups may interact strongly with guest molecules, essentially mimicking a solvation-like effect. Accordingly, a series of linker molecules with pendant C3 alkoxy groups were prepared. Various degrees of branching and saturation could be expected to differentially adsorb or "dissolve" methane, ethane, ethylene, or acetylene.

A MOF particularly amenable to the introduction of various ligand molecules is the pillared framework Zn_2(fu-bdc)$_2$(dabco) (fu-bdc^{2-} = 2,5-functionalized-1,4-benzenedicarboxylate; dabco = 1,4-diazabicyclo[2.2.2]octane; Figure 1). Frameworks of this type have shown interesting properties, such as tunable framework flexibility upon solvent and gas adsorption/desorption or in response to temperature changes.[15] This family of frameworks is derived from the well-studied, archetypal pillared-layered framework $Zn_2(bdc)_2$(dabco) (bdc^{2-} = 1,4-benzenedicarboxylate), which consists of Zn_2 paddlewheel units interconnected by 1,4-benzenedicarboxylate linkers to form a two-dimensional $Zn_2(bdc)_2$ grid.[16] These grids are extended into a three-dimensional structure with the pillaring ligand dabco. In the functionalized analogue, Zn_2(fu-bdc)$_2$(dabco), a phase transition occurs upon activation, from the as-synthesized large-pore form (**lp**) to the activated narrow-pore form (**np**; Figure 1b). This phenomenon is often referred to as a "breathing effect".[17] The phase transition initiated by guest removal/reintroduction is attributed to the sidechains attached to the linker molecule. When the pore is filled with guest molecules, the pendant sidechains interact with the guests, which leads to the **lp** phase. After removal of the guest, a contraction of the Zn_2(fu-bdc)$_2$ grid, initiated by favorable interactions between neighboring sidechains, occurs. The square framework structure is transformed into a rhombic framework structure that leaves the dabco-containing axis unaffected. The resulting **np** phase possesses a substantially lower unit cell volume (see Figure S7 in the Supporting Information for the cell volumes of activated compounds **1**–**4**). In the **np** phase, the pore entrances are lined by the "solvent-like" sidechains on the linker, which leads to a maximum interaction of the sidechains with potential guest molecules.[15c] The magnitude of the pore contraction initiated by the guest removal highly depends on the nature of the sidechains. For example, substantial differences in the CO_2 adsorption isotherms at 195 K were observed for different functionalized linkers, which makes it possible to tune the uptake and the CO_2 phase transition pressure back to the **lp** form.[15c,e]

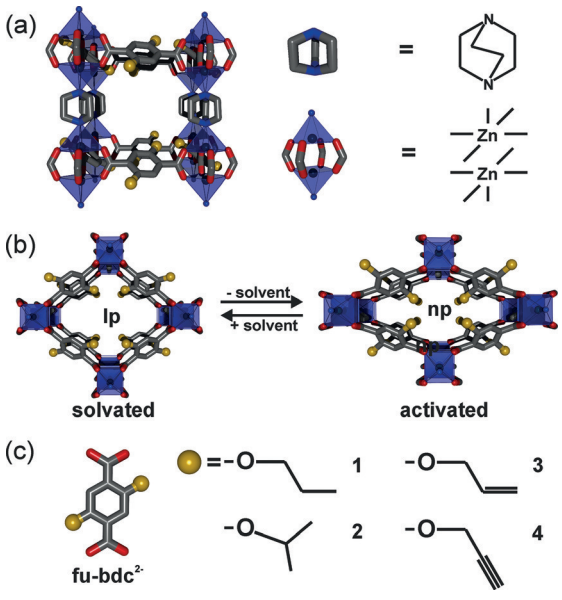

Figure 1. a) Side view of a single cavity and sketch of the framework building units. b) Schematic depiction of a single cavity of a pillared-layered metal–organic frameworks of the type Zn_2(fu-bdc)$_2$(dabco) in the solvated state (**lp**) and the activated state (**np**). Carbon: grey, oxygen: red, nitrogen: blue, zinc: dark green; coordination spheres around the Zn are represented by blue polyhedra. c) Representation of the chemical structures of the H_2fu-bdc linker molecules used for the preparation of MOFs **1**–**4**.

Results and Discussion

To potentially endow Zn_2(fu-bdc)$_2$(dabco) with selectivity for specific light hydrocarbons, four different H_2fu-bdc molecules were selected: H_2DP-bdc (2,5-dipropoxy-1,4-benzenedicarboxylic acid), H_2DiP-bdc (2,5-diisopropoxy-1,4-benzenedicarboxylic acid), H_2BA-bdc (2,5-bis(allyloxy)-1,4-benzenedicarboxylic acid), and H_2BPy-bdc (2,5-bis(prop-2-ynyloxy)-1,4-benzenedicarboxylic acid; Figure 2). By using standard solvothermal methods (details can be found in the Experimental Section), we synthesized the functionalized frameworks Zn_2(DP-bdc)$_2$(dabco) (**1**), Zn_2(DiP-bdc)$_2$(dabco) (**2**), Zn_2(BA-bdc)$_2$(dabco) (**3**), and Zn_2(BPy-bdc)$_2$(dabco) (**4**). Upon evacuation of solvent-exchanged materials at elevated temperatures, the frameworks are all present in their **np** forms, as determined by powder X-ray diffraction and gas adsorption analysis (see Figures S5, S6, S10, and S11 in the Supporting Information).

Adsorption isotherms for methane, ethane, ethylene, and acetylene were measured at 298 K for compounds **1**–**4** (Figure 2). The trend in adsorption capacity at 1 bar is the same for all four materials, with $CH_4 < C_2H_6 \approx C_2H_4 < C_2H_2$. Under these conditions, **1** and **2** display the lowest acetylene uptake of 0.34 and 0.23 mmol g^{-1}, respectively. Interestingly, the materials with fu-bdc linkers that contain alkene and alkyne functionalities adsorb significantly more acetylene, with

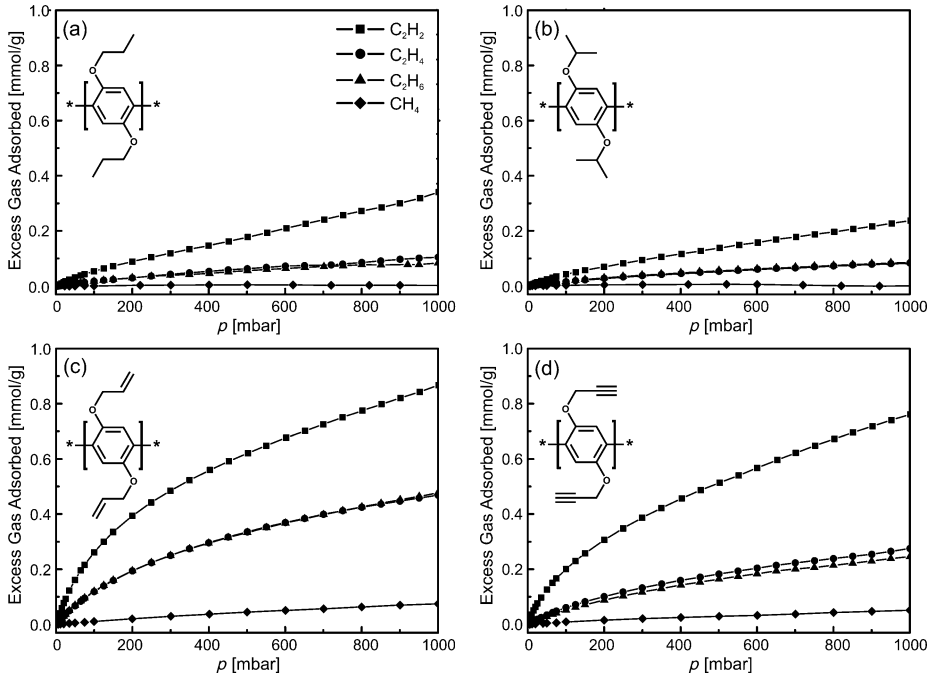

Figure 2. Adsorption isotherms for CH_4 (◆), C_2H_6 (▲), C_2H_4 (●), and C_2H_2 (■) measured at 298 K for a) **1**, b) **2**, c) **3**, and d) **4**.

3 and **4** displaying capacities of 0.87 and 0.76 mmol g^{-1}, respectively, at 1 bar. At similar pressures, **1** and **2** display low ethylene and ethane uptakes of approximately 0.1 mmol g^{-1}, whereas **3** and **4** have moderate uptakes of 0.47 and 0.25 mmol g^{-1}, respectively. The methane uptake in all four cases is very low, ranging from 0.001 to 0.07 mmol g^{-1}.

All the isotherms measured display typical type I behavior, which confirms that the materials remain in the **np** form during the adsorption of hydrocarbons under these conditions (298 K, 0–1 bar). This observation is in distinct contrast to the low-temperature CO_2 isotherms of the same materials that feature a distinct step in the uptake curve of the isotherm, which indicates a pore transformation from **np** to **lp**.[15c] In principle, a similar phase transition during the adsorption of light hydrocarbons is also possible, though it likely occurs at higher pressures and/or lower temperatures than studied here. To exclude the effects of pore size as the driving force for the adsorption of certain hydrocarbons, the powder X-ray diffraction patterns of activated materials **1**–**4** were fit by using the Pawley method[18] and the unit cell parameters were obtained (see Figure S7 in the Supporting Information). The fits confirm that all four materials are present in their **np** form, with moderately different unit cell volumes. Thus, slight variations in accessible pore volume as a function of the functionality on the bdc^{2-} linker are anticipated.

Interestingly, the trend in the decrease in cell volume of the **np** materials **1**–**4** ($V_1 \approx V_2 > V_3 > V_4$) does not match with the trends in guest uptake observed from the physisorption measurements. Therefore, the dissimilarities in gas uptake capacities are induced primarily by differences in substituent–guest interactions. The adsorption capacities at 298 K and 1 bar suggest that the different adsorption capacities are not based on a sieving effect because the kinetic diameters of the molecules investigated follow the trend $C_2H_6 > C_2H_4 > CH_4 > C_2H_2$. In addition, the polarizabilities of the molecules increase from methane to ethane, with $CH_4 < C_2H_2 < C_2H_4 < C_2H_6$ (see Table S1 in the Supporting Information). Thus, it is most likely that significant π–π interactions of C_2H_2 with the sidechains lead to the higher uptake (**3** and **4**). Nevertheless, it needs to be noted that the C_2H_4 and C_2H_6 uptake are nearly identical, which suggests that the observed differences in uptake cannot be solely based on the variation in π–π interactions of the adsorbents with the sidechains. Although the overall adsorption capacities are perhaps somewhat low in comparison to other MOFs (for example, the parent material $Zn_2(bdc)_2(dabco)$ without the flexible sidechains takes up approximately 4.2 mmol g^{-1} of C_2H_2[19] and 7.5 mmol g^{-1} of CH_4[20] at 298 and 296 K, respectively), a high relative difference between the acetylene and ethylene uptake is apparent, which indicates a comparably strong selectivity for the adsorption of acetylene.

Typical gas adsorption analyzers measure only single-component isotherms and the routine measurement of binary gas mixtures is complicated. A model that can reliably determine adsorption selectivity for mixed gas systems was developed by Myers and Prausnitz.[21] Their ideal adsorbed solution theory (IAST) can be used to estimate selectivity coefficients, which are defined by the equation

$$S_{ads} = \frac{x_1/x_2}{y_1/y_2}$$

in which S_{ads} is the adsorption selectivity, x_i is the amount of adsorbed gas as determined using IAST, and y_i is the mole fraction of each component in the gas phase at equilibrium. The calculated selectivities are displayed in Figure 3. Consistent with the high acetylene uptake exhibited by **4**, this material has the highest C_2H_2/C_2H_6, selectivity, with a value of 7.3 for an equimolar mixture at 1 bar and 298 K, whereas **1**, **2**, and **3** display selectivities of 6.2, 3.7, and 3.2, respectively. The somewhat lower selectivity obtained for **3** could potentially be explained by a partially ordered alignment of the allyloxy sidechains inside the pores that leads to an increase in the number of freely accessible adsorption sites, and thus increases the uptake for all four adsorbates. This is in agreement with the observation that **3** is the only material under study here that adsorbs reasonable amounts of N_2 at 77 K (≈40 cm^3 g^{-1}),

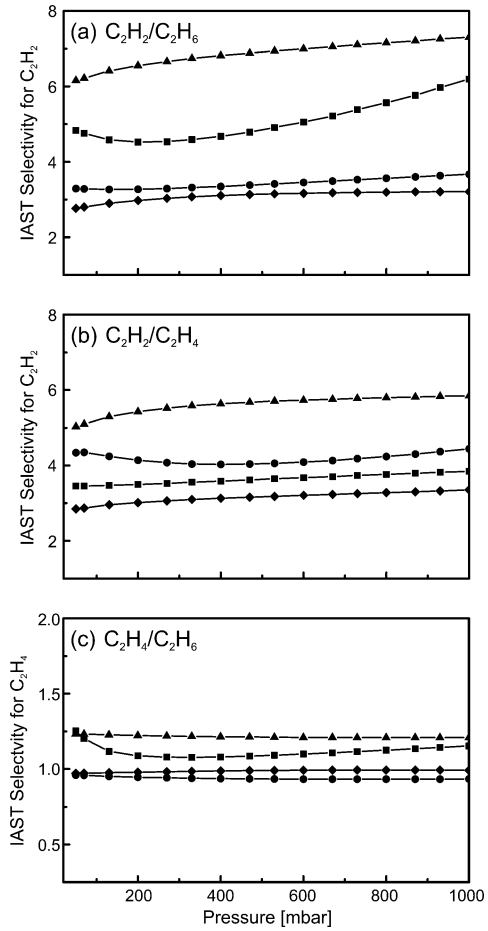

Figure 3. Selectivity factors for **1** (■), **2** (●), **3** (◆), and **4** (▲) for the separation of 50:50 mixtures of a) C_2H_2/C_2H_6, b) C_2H_2/C_2H_4, and c) C_2H_4/C_2H_6 at 298 K.

whereas the other materials are essentially nonporous towards N_2.[15c]

The C_2H_2/C_2H_4 selectivity factors are slightly lower than those for C_2H_2/C_2H_6. For an equimolar mixture at 1 bar total pressure, selectivities of 5.9, 4.4, and 3.8 are observed for **4**, **1**, and **2**, respectively. The selectivity of **4** represents, to our knowledge, the highest reported selectivity for an equimolar acetylene/ethylene mixture at 1 bar of total pressure and 298 K, and is only rivaled by the selectivity of M′MOF-3 (5.2).[10a] Again, the lowest selectivity is found for **3**, with a value of 3.4. This value, however, is still among the highest reported for metal–organic frameworks under these conditions. Indeed, two widely studied metal–organic frameworks, Fe_2(dobdc) and NOTT-300, display selectivities of 2.2 (at 318 K) and 2.3 (at 293 K), respectively.[22]

Because there is utility in removing trace acetylene impurities from ethylene streams, we also evaluated selectivity for 1:99 C_2H_2/C_2H_4 mixtures. Particularly high values were recently reported for M′MOF-3[10a] and UTSA-100a,[23] which show selectivities of 24.0 and 10.7, respectively, whereas the selectivities of NOTT-300 (2.2) and Fe_2(dobdc) (2.1) were considerably lower.[23] For material **4**, the IAST value for a 1:99 C_2H_2/C_2H_4 mixture at 1 bar is 5.6, which makes it, to the best of our knowledge, the third-best material reported for this set of parameters (see Table 1 for selectivities for 1:99 and 99:1 mixtures at 1 bar).

Table 1. IAST selectivity calculated for materials **1**–**4** for C_2H_2/C_2H_4 mixtures with ratios of 1:99, 50:50, and 99:1 at 1 bar and 298 K.

Material	1:99	50:50	99:1
1	4.0	4.4	5.4
2	3.6	3.8	4.0
3	3.2	3.4	3.6
4	5.6	5.9	6.0

Conclusion

In addition to the commonly employed methods of modifying uptake and selectivity for short-chained hydrocarbons in metal–organic frameworks, the foregoing results demonstrate that linker functionalization with flexible sidechains can effectively be used to tune adsorption selectivity for specific hydrocarbons. The highest uptake of unsaturated hydrocarbons occurred in Zn_2(fu-bdc)$_2$(dabco) materials with unsaturated sidechains. The high acetylene uptake and C_2H_2/C_2H_4 selectivity can be credited to strong π–π interactions, which apparently give rise to additional adsorption sites. Ethane and ethylene are moderately adsorbed at a very similar level, this might be induced by the much weaker π–π interactions of the ethylene (compared with acetylene) and the van der Waals interactions/polarizability of the ethane that balance each other out. Given the modular nature of MOFs, this strategy should be generally applicable and transferable to the vast field of 1,4-benzenedicarboxylate-based frameworks and beyond. The issue of low overall capacities may be overcome by using larger pore structures or perhaps through the preparation of suitable core–shell systems.[24] Future investigations will expand the library of H_2fu-bdc linkers and employ them in the synthesis of a wide array of prototypical MOFs. More sophisticated tuning of separation properties could potentially be achieved through the synthesis of solid–solution MOFs that contain several different linkers,[25] or through the implementation of these new MOFs in membranes[26] and thin-film devices.[27]

Experimental Section

Materials

All chemicals were purchased from commercial suppliers (Sigma–Aldrich, Fluka, Alfa Aesar, ABCR, and others) and used without further purification. The tetrahydrofuran (THF) used in the linker synthesis was catalytically dried, deoxygenated, and saturated with argon by using an automatic solvent purification system from MBraun. The residual water content was determined by using Karl Fischer titration, which indicated levels of 5 ppm. The activated MOF samples were stored under argon in a glovebox (MBraun LabStar) before further measurements.

Methods

For the adsorption measurements, samples **1**–**4** (150–200 mg) were transferred into a pre-weighed sample tube under nitrogen and capped with a Transeal. The samples were then outgassed on the activation unit of a Micromeritics ASAP 2020 gas adsorption analyzer and heated at a rate of 0.1 K min^{-1} from RT to 433 K. When the outgas rate was below 2 μbar min^{-1}, the samples were considered fully activated. The evacuated tubes were subsequently weighed again to determine the measurement weight, then the samples were transferred to the analysis port of the Micromeritics 2020 instrument and again heated to 433 K and evacuated until the outgas rate was below 2 μbar min^{-1}. Isothermal conditions were ensured by using a recirculating dewar connected to an isothermal bath. The gases used for measurements had purities of 99.5% for acetylene and 99.99% or higher for methane, ethane, ethylene, nitrogen, CO_2, and H_2. Liquid-phase NMR spectra were recorded by using a Bruker Advance DPX 200 spectrometer (^{1}H, 200 MHz) or a Bruker Advance DPX 250 spectrometer (^{1}H, 250 MHz) at 293 K. ^{1}H NMR spectra of the synthesized linker molecules were recorded in [D_6]DMSO and the spectra of digested MOFs were recorded in 0.5 mL [D_6]DMSO and 0.05 mL of DCl/D_2O (20%). Chemical shifts are given relative to TMS and referenced to the solvent signals as internal standards. Infrared spectra were recorded by using a Bruker Alpha-P FT-IR situated in a glovebox. For all measurements the ATR mode of the spectrometer was used and measurements with 48 scans were performed. All thermogravimetric analyses (TGA) were performed by using a Netzsch STA 409 PC TG-DSC apparatus. A heating rate of 5 K min^{-1} was applied and the samples were placed in clean pre-weighed aluminum oxide crucibles. All measurements were performed in a stream of N_2 gas with a constant flow rate of 20 mL min^{-1}. Powder X-ray diffraction (PXRD) measurements were performed by using a PanAlytical X'Pert Pro with $Cu_{K\alpha}$ radiation in Bragg–Brentano geometry with an automatic divergence slit and a position-sensitive detector in continuous scan mode in the range of $2\theta = 5$–50°. The samples were measured on zero-background silica substrates cut along the [510] plane. For measurements of the as-synthesized samples, the MOF powders were taken straight from the synthesis solution and measured while still slightly wet from the solvent. For measurements of the dried samples, the substrate was covered with a thin film of grease and the dried samples were distributed on the grease.

Linker synthesis

The linkers H_2DP-bdc, H_2DiP-bdc, H_2BA-bdc, and H_2BPy-bdc were prepared according to known literature procedures.[15c]

Synthesis of Zn_2(fu-bdc)$_2$(dabco) (1–4)

H_2fu-bdc (H_2DP-bdc, H_2DiP-bdc, H_2BA-bdc, or H_2BPy-bdc, respectively; 1.5 mmol), dabco (90 mg, 0.8 mmol), and $Zn(NO_3)_2 \cdot 6H_2O$ (446.2 mg, 1.5 mmol) were placed in a beaker, *N*,*N*-dimethylformamide (DMF; 30 mL) was added, and the mixture was sonicated until everything was dissolved. The mixture was left for 10 min to settle and a precipitate formed. The precipitate was filtered off and the filtrate was collected in a screw jar, sealed, and placed in an oven at 120 °C for 48 h. Next, the vessel was slowly cooled to RT and the solvent was decanted and fresh DMF was added. A stirring bar was added and the content of the reaction vessel was stirred for 30 min. The mixture was left to stand for 24 h and the solvent was exchanged twice for $CHCl_3$, followed by 30 min of stirring, over the course of 48 h. Afterwards the MOF powder was filtered off and transferred to a Schlenk flask and dried at 120 °C in vacuo (oil pump). The dried material was then stored under argon in a glovebox. NMR spectra, powder XRD, TG, IR, and adsorption measurements (CO_2, N_2, and H_2) of the materials can be found in the Supporting Information.

Acknowledgements

A.S. gratefully acknowledges the research cluster SusChemSys for a doctoral fellowship. The project "Sustainable Chemical Synthesis (SusChemSys)" is co-financed by the European Regional Development Fund (ERDF) and the state of North Rhine-Westphalia, Germany, under the Operational Programme "Regional Competitiveness and Employment" 2007–2013. A.S. and R.A.F. are also grateful for support from the Cluster of Excellence RESOLV (EXC1069) funded by the Deutsche Forschungsgemeinschaft. Gas adsorption measurements and data analysis was supported by the Center for Gas Separations Relevant to Clean Energy Technologies, an Energy Frontier Research Center funded by the U.S. Department of Energy, Office of Science, Office of Basic Energy Sciences under award DE-SC0001015. We further thank Gerald K. Branch and Arkema for fellowship support of E.D.B. and the Alexander von Humboldt Foundation for providing S.H. with a Feodor Lynen Return Fellowship.

Keywords: host–guest systems · hydrocarbons · linker functionalization · metal–organic frameworks

[1] P. Pässler, W. Hefner, K. Buckl, H. Meinass, A. Meiswinkel, H.-J. Wernicke, G. Ebersberg, R. Müller, J. Bässler, H. Behringer, D. Mayer, in *Ullmann's Encyclopedia of Industrial Chemistry*, Wiley-VCH Verlag GmbH & Co. KGaA, **2000**.

[2] R. B. Eldridge, *Ind. Eng. Chem. Res.* **1993**, *32*, 2208–2212.

[3] Z. R. Herm, E. D. Bloch, J. R. Long, *Chem. Mater.* **2014**, *26*, 323–338.

[4] a) Metal–organic frameworks special issue, *Chem. Soc. Rev.* **2009**, *38*, 1213–1477; b) Metal–organic frameworks special issue, *Chem. Rev.* **2012**, *112*, 673–1268; c) Metal–organic frameworks special issue, *Chem. Soc. Rev.* **2014**, *43*, 5415–6172.

[5] a) H. Furukawa, K. E. Cordova, M. O'Keeffe, O. M. Yaghi, *Science* **2013**, *341*, 1230444; b) M. Li, D. Li, M. O'Keeffe, O. M. Yaghi, *Chem. Rev.* **2014**, *114*, 1343–1370; c) W. Lu, Z. Wei, Z.-Y. Gu, T.-F. Liu, J. Park, J. Park, J. Tian, M. Zhang, Q. Zhang, T. Gentle III, M. Bosch, H.-C. Zhou, *Chem. Soc. Rev.* **2014**, *43*, 5561–5593; d) A. Schneemann, S. Henke, I. Schwedler, R. A. Fischer, *ChemPhysChem* **2014**, *15*, 823–839; e) H. Furukawa, U. Mueller, O. M. Yaghi, *Angew. Chem. Int. Ed.* **2015**, *54*, 3417–3430; *Angew. Chem.* **2015**, *127*, 3480–3494; f) A. G. Slater, A. I. Cooper, *Science* **2015**, *348*, aaa8075.

[6] a) S. Xiang, W. Zhou, Z. Zhang, M. A. Green, Y. Liu, B. Chen, *Angew. Chem. Int. Ed.* **2010**, *49*, 4615–4618; *Angew. Chem.* **2010**, *122*, 4719–4722; b) E. D. Bloch, W. L. Queen, R. Krishna, J. M. Zadrozny, C. M. Brown, J. R. Long, *Science* **2012**, *335*, 1606–1610; c) Y.-S. Bae, C. Y. Lee, K. C. Kim, O. K. Farha, P. Nickias, J. T. Hupp, S. T. Nguyen, R. Q. Snurr, *Angew. Chem. Int. Ed.* **2012**, *51*, 1857–1860; *Angew. Chem.* **2012**, *124*, 1893–1896; d) S. J. Geier, J. A. Mason, E. D. Bloch, W. L. Queen, M. R. Hudson, C. M. Brown, J. R. Long, *Chem. Sci.* **2013**, *4*, 2054–2061; e) X. Duan, Y. He, Y. Cui, Y. Yang, R. Krishna, B. Chen, G. Qian, *RSC Adv.* **2014**, *4*, 23058–23063; f) X. Duan, R. Song, J. Yu, H. Wang, Y. Cui, Y. Yang, B. Chen, G. Qian, *RSC Adv.* **2014**, *4*, 36419–36424.

[7] a) B. Chen, C. Liang, J. Yang, D. S. Contreras, Y. L. Clancy, E. B. Lobkovsky, O. M. Yaghi, S. Dai, *Angew. Chem. Int. Ed.* **2006**, *45*, 1390–1393; *Angew. Chem.* **2006**, *118*, 1418–1421; b) C. Gücüyener, J. van den Bergh, J. Gascon, F. Kapteijn, *J. Am. Chem. Soc.* **2010**, *132*, 17704–17706; c) Y. He,

S. Xiang, B. Chen, *J. Am. Chem. Soc.* **2011**, *133*, 14570 – 14573; d) H. Bux, C. Chmelik, R. Krishna, J. Caro, *J. Membr. Sci.* **2011**, *369*, 284 – 289; e) Y. He, Z. Zhang, S. Xiang, H. Wu, F. R. Fronczek, W. Zhou, R. Krishna, M. O'Keeffe, B. Chen, *Chem. Eur. J.* **2012**, *18*, 1901 – 1904; f) Y. Pan, T. Li, G. Lestari, Z. Lai, *J. Membr. Sci.* **2012**, *390 – 391*, 93 – 98; g) N. Nijem, H. Wu, P. Canepa, A. Marti, K. J. Balkus, T. Thonhauser, J. Li, Y. J. Chabal, *J. Am. Chem. Soc.* **2012**, *134*, 15201 – 15204; h) M. G. Plaza, A. F. P. Ferreira, J. C. Santos, A. M. Ribeiro, U. Mueller, N. Trukhan, J. M. Loureiro, A. E. Rodrigues, *Microporous Mesoporous Mater.* **2012**, *157*, 101 – 111; i) U. Böhme, B. Barth, C. Paula, A. Kuhnt, W. Schwieger, A. Mundstock, J. Caro, M. Hartmann, *Langmuir* **2013**, *29*, 8592 – 8600; j) K. Liu, B. Li, Y. Li, X. Li, F. Yang, G. Zeng, Y. Peng, Z. Zhang, G. Li, Z. Shi, S. Feng, D. Song, *Chem. Commun.* **2014**, *50*, 5031 – 5033; k) N. A. Ramsahye, P. Trens, C. Shepherd, P. Gonzalez, T. K. Trung, F. Ragon, C. Serre, *Microporous Mesoporous Mater.* **2014**, *189*, 222 – 231; l) H. Alawisi, B. Li, Y. He, H. D. Arman, A. M. Asiri, H. Wang, B. Chen, *Cryst. Growth Des.* **2014**, *14*, 2522 – 2526.

[8] a) V. R. Choudhary, S. Mayadevi, *Zeolites* **1996**, *17*, 501 – 507; b) W. Zhu, F. Kapteijn, J. A. Moulijn, M. C. Den Exter, J. C. Jansen, *Langmuir* **2000**, *16*, 3322 – 3329; c) D. H. Olson, M. A. Camblor, L. A. Villaescusa, G. H. Kuehl, *Microporous Mesoporous Mater.* **2004**, *67*, 27 – 33.

[9] Z. R. Herm, B. M. Wiers, J. A. Mason, J. M. van Baten, M. R. Hudson, P. Zajdel, C. M. Brown, N. Masciocchi, R. Krishna, J. R. Long, *Science* **2013**, *340*, 960 – 964.

[10] a) S.-C. Xiang, Z. Zhang, C.-G. Zhao, K. Hong, X. Zhao, D.-R. Ding, M.-H. Xie, C.-D. Wu, M. C. Das, R. Gill, K. M. Thomas, B. Chen, *Nat. Commun.* **2011**, *2*, 204; b) M. C. Das, Q. Guo, Y. He, J. Kim, C.-G. Zhao, K. Hong, S. Xiang, Z. Zhang, K. M. Thomas, R. Krishna, B. Chen, *J. Am. Chem. Soc.* **2012**, *134*, 8703 – 8710.

[11] a) Z. Zhang, S. Xiang, K. Hong, M. C. Das, H. D. Arman, M. Garcia, J. U. Mondal, K. M. Thomas, B. Chen, *Inorg. Chem.* **2012**, *51*, 4947 – 4953; b) J. Cai, J. Yu, H. Xu, Y. He, X. Duan, Y. Cui, C. Wu, B. Chen, G. Qian, *Cryst. Growth Des.* **2013**, *13*, 2094 – 2097.

[12] G. E. Cmarik, M. Kim, S. M. Cohen, K. S. Walton, *Langmuir* **2012**, *28*, 15606 – 15613.

[13] S. Henke, R. A. Fischer, *J. Am. Chem. Soc.* **2011**, *133*, 2064 – 2067.

[14] J. Seo, R. Matsuda, H. Sakamoto, C. Bonneau, S. Kitagawa, *J. Am. Chem. Soc.* **2009**, *131*, 12792 – 12800.

[15] a) S. Henke, R. Schmid, J.-D. Grunwaldt, R. A. Fischer, *Chem. Eur. J.* **2010**, *16*, 14296 – 14306; b) S. Henke, D. C. F. Wieland, M. Meilikhov, M. Paulus, C. Sternemann, K. Yusenko, R. A. Fischer, *CrystEngComm* **2011**, *13*, 6399 – 6404; c) S. Henke, A. Schneemann, A. Wuetscher, R. A. Fischer, *J. Am. Chem. Soc.* **2012**, *134*, 9464 – 9474; d) S. Henke, A. Schneemann, R. A. Fischer, *Adv. Funct. Mater.* **2013**, *23*, 5990 – 5996; e) V. Bon, J. Pallmann, E. Eisbein, H. C. Hoffmann, I. Senkovska, I. Schwedler, A. Schneemann, S. Henke, D. Wallacher, R. A. Fischer, G. Seifert, E. Brunner, S. Kaskel, *Microporous Mesoporous Mater.* **2015**, *216*, 64 – 74.

[16] D. N. Dybtsev, H. Chun, K. Kim, *Angew. Chem. Int. Ed.* **2004**, *43*, 5033 – 5036; *Angew. Chem.* **2004**, *116*, 5143 – 5146.

[17] a) G. Férey, C. Serre, *Chem. Soc. Rev.* **2009**, *38*, 1380 – 1399; b) S. Horike, S. Shimomura, S. Kitagawa, *Nat. Chem.* **2009**, *1*, 695 – 704; c) A. Schneemann, V. Bon, I. Schwedler, I. Senkovska, S. Kaskel, R. A. Fischer, *Chem. Soc. Rev.* **2014**, *43*, 6062 – 6096.

[18] G. S. Pawley, *J. Appl. Crystallogr.* **1981**, *14*, 357 – 361.

[19] D. Tanaka, M. Higuchi, S. Horike, R. Matsuda, Y. Kinoshita, N. Yanai, S. Kitagawa, *Chem. Asian J.* **2008**, *3*, 1343 – 1349.

[20] H. Kim, D. G. Samsonenko, S. Das, G.-H. Kim, H.-S. Lee, D. N. Dybtsev, E. A. Berdonosova, K. Kim, *Chem. Asian J.* **2009**, *4*, 886 – 891.

[21] A. L. Myers, J. M. Prausnitz, *AIChE J.* **1965**, *11*, 121 – 127.

[22] S. Yang, A. J. Ramirez-Cuesta, R. Newby, V. Garcia-Sakai, P. Manuel, S. K. Callear, S. I. Campbell, C. C. Tang, M. Schröder, *Nat. Chem.* **2014**, *7*, 121 – 129.

[23] T.-L. Hu, H. Wang, B. Li, R. Krishna, H. Wu, W. Zhou, Y. Zhao, Y. Han, X. Wang, W. Zhu, Z. Yao, S. Xiang, B. Chen, *Nat. Commun.* **2015**, *6*, 7328.

[24] K. Hirai, S. Furukawa, M. Kondo, H. Uehara, O. Sakata, S. Kitagawa, *Angew. Chem. Int. Ed.* **2011**, *50*, 8057 – 8061; *Angew. Chem.* **2011**, *123*, 8207 – 8211.

[25] a) A. D. Burrows, *CrystEngComm* **2011**, *13*, 3623 – 3642; b) Y.-B. Zhang, H. Furukawa, N. Ko, W. Nie, H. J. Park, S. Okajima, K. E. Cordova, H. Deng, J. Kim, O. M. Yaghi, *J. Am. Chem. Soc.* **2015**, *137*, 2641 – 2650.

[26] a) J.-R. Li, R. J. Kuppler, H.-C. Zhou, *Chem. Soc. Rev.* **2009**, *38*, 1477 – 1504; b) J.-R. Li, J. Sculley, H.-C. Zhou, *Chem. Rev.* **2012**, *112*, 869 – 932.

[27] a) A. Bétard, R. A. Fischer, *Chem. Rev.* **2012**, *112*, 1055 – 1083; b) M. Tu, S. Wannapaiboon, R. A. Fischer, *Inorg. Chem. Front.* **2014**, *1*, 442 – 463.

Received: September 14, 2015
Published online on November 12, 2015